18TH WORLD CONFERENCE ON EARTHQUAKE ENGINEERING
WCEE2024
MILAN

MILAN, ITALY
30TH JUNE - 5TH JULY 2024
www.wcee2024.it

EARTHQUAKE AND TSUNAMI MULTI-HAZARD NATECH RISK ASSESSMENT FOR PETROCHEMICAL STORAGE FACILITIES

A. Vitale[1], G. Baltzopoulos[1] & I. Iervolino[1,2]

[1] Università degli Studi di Napoli Federico II, Naples, Italy,

{antonio.vitale5, georgios.baltzopoulos, iunio.iervolino}@unina.it

[2] IUSS – Scuola Universitaria Superiore di Pavia, Pavia, Italy

Abstract: *Industrial accidents can occur triggered by natural hazard events, where phenomena such as earthquakes, tsunamis or hurricanes, can lead to structural damage of storage facilities and/or piping. That may then cause the release of hazardous substances, initiating a chain of cascading effects, potentially involving fire, blasts, or toxic pollution. The term NaTech has been introduced to describe such natural-hazard-triggered technological accidents. This article presents a possible multi-hazard NaTech risk assessment for process industry plants accounting for earthquakes and tsunamis. A hypothetical waterfront liquefied petroleum gas tank farm situated at a coastal Italian site is considered, as a representative module of an oil refinery. The risk assessment uses steel storage tank fragility functions for earthquake ground shaking and tsunami waves, which depend on each tank's filling level of the tanks. These are integrated with seismic shaking and tsunami inundation hazard curves for the site considered, to provide the annual rate of tank failure, where failure is defined as structural damage able to cause release of contents.*

1 Introduction

Natural hazards, such as earthquakes, floods, hurricanes, or tsunamis can trigger technological accidents (NaTech) in industrial facilities. Technological accidents, causing structural damage to industrial units or the detachment of pipelines, can be followed by the release of highly flammable or otherwise hazardous substances that can, in turn, lead to a series of hazardous events such as explosions, pool fire or toxic pollution. In this context, the assessment of the risk, to which industrial facilities are exposed due to natural hazards, becomes necessary in order to make informed decisions about measures of risk mitigation and reduction.

Guidelines on quantitative NaTech risk assessment (QRA) are present in the literature (Lees and Lees, 2005; Center for Chemical Process Safety (CCPS), 2010) and have found application in several works (Cozzani et al., 2014; Fabbrocino et al., 2005). The implementation of QRA typically requires mathematical models that provide the conditional probability of damage to industrial installations, given the manifestation of a natural hazard of specific intensity, known as *fragility models*. Thus, the number and variety of different structures featured in an industrial facility can present a challenge, as the analyst may be hard-pressed to obtain appropriate fragility models from the literature to cover their entirety. For this reason, it may be necessary for a QRA to pool together fragility models developed via different approaches, such as empirical fragility calibrated against data from past industrial accidents triggered from historical natural hazard events, for example earthquakes (Salzano, Iervolino and Fabbrocino, 2003), or analytical fragilities based on simplified structural models, such as those derived in a past work for some types of storage tanks under tsunami events (Basco and Salzano, 2016).

The study presented in this paper considers NaTech risk analysis in the face of two natural hazards: earthquakes and tsunamis. On-purpose developed analytical fragility models for anchored atmospheric storage tanks subjected to tsunamis are applied to evaluate the annual rate of structural damages that may lead to potential content release, for a number of case-study situations. This rate is a risk metric that can be used to carry out consequence analysis in QRA. In each case-study, existing seismic fragility models from the literature are used to provide an additional risk assessment against earthquake-induced ground shaking, for comparison. In both cases, the same seismic source models underlie the hazard analysis for both natural hazards. This analysis is repeated for several tank geometries, at the same coastal site, and various assumptions concerning the amount of liquid contents found in tanks. The resulting failure rates are then compared and discussed.

2 Risk assessment

2.1 Case-study scenarios

Tsunami and earthquake risk analysis is performed for a series of anchored atmospheric storage tanks, belonging to a hypothetical petrochemical refinery located on the waterfront. The two natural hazards risks are herein examined separately to enable comparisons, although these results could be regarded as part of a NaTech multi-risk analysis. Three case-studies are considered, in terms of tank geometry, so the evaluation of structural failure rate is performed for tanks with three different height-to-radius ratios.

The assumed site for these case-studies is in Sicily (Southern of Italy), on its Thyrrenean Sea coast. For this site, probabilistic tsunami hazard analysis (PTHA) has been already conducted in a previous work (Volpe *et al.*, 2019), while a probabilistic seismic hazard analysis (PSHA), based on the same seismic source models as the tsunami hazard, was performed by the authors of the present paper, along the lines of classical procedures (Cornell, 1968), with the results and details on methodology available in a separate publication (Vitale, 2024). The hazard at the site, for both natural events, is expressed in terms of exceedance rate, that is the mean annual frequency of events that cause exceedance of a certain event intensity threshold at the site. Herein, the tsunami intensity is measured in terms of the maximum tsunami height (h_w), while the chosen intensity measure (im) for the seismic ground motion is the peak ground acceleration (*pga*). The PTHA was developed though numerical simulations of inundation scenarios triggered by seismic events and the results were made available for the present study by Volpe and co-authors(Volpe *et al.*, 2019), for a grid of points covering an area around the alleged refinery. For the interest of this case study, only the tsunami hazard associated a single point from that grid is considered, and the various analysed tanks are ideally placed in that location, in the interest of comparison. The results of the PTHA and PSHA are shown in Fig.1, under the form of hazard curves, that plot the exceedance rates of various *pga* values (λ_{pga}) for the seismic case and of h_w values (λ_{h_w}) for the tsunami case. (Note that the initial tract of the λ_{pga} curves is not shown, in order to facilitate representation of both using the same scale for the ordinate, because the λ_{h_w} hazard at this site is generally lower than the seismic one).

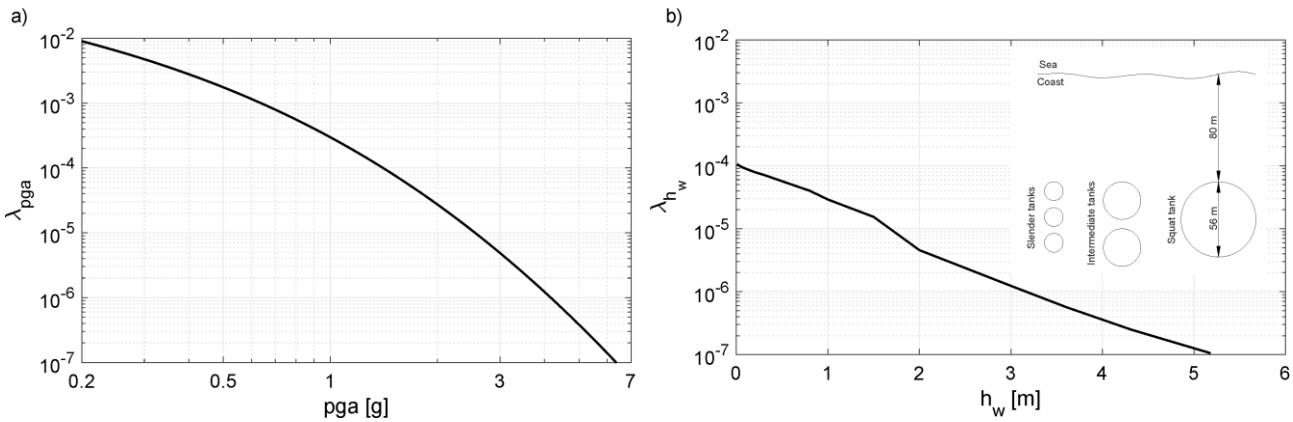

Fig.1. (a) seismic and (b) tsunami hazard curves for the case-study site.

The examined atmospheric storage tanks are cylindrical steel shell structures, anchored along the perimeter on a concrete foundation mat, and equipped with a floating roof that moves along guide stanchions with the

level of the liquid content, that is, a type of tank that is typically used to store gasoil or fuel oil. The assumption for the detailing of the shell and base plate thicknesses, as well as the anchorage system, is that these tanks are representative of modern code-conforming structures designed for earthquake resistance (UNI EN 1993-1-8, 2005; UNI EN 1998-4, 2006; UNI EN 1993-4-2, 2017; API 650, 2018). Three tank geometries are considered here, that differ in aspect ratio, which is defined as the ratio the height (H) and the radius of the tank (R). Herein, the tanks are classified as: slender with $H/R = 2$; intermediate with $H/R = 1$; squat with $H/R = 0.5$.

2.2 Fragility models

Structural vulnerability to natural hazards can be quantified by so-called fragility functions, that express the probability of exceeding a damage state or performance level, given a measure of the event's intensity manifest at the site of interest. In the context of this work, the performance level considered is that of the natural hazard event causing enough structural damage to the tank to provoke the release of its contents, hereafter termed *failure* for brevity. Factors that can influence the behaviour of a storage tank under seismic or tsunami loads include the geometry, filling level, and the anchorage condition at the base. Observations collected in the aftermath of past events, have shown that types of damage experienced by anchored steel tanks can include tension or shear failure of the anchor bolts, connecting pipelines' failure due to large vertical or horizontal displacements when the tank is subjected to base uplifting or sliding, or large deformations of the shell in proximity of the base plate or the roof, due to the dynamic motion of the liquid mass inside the tank, or shell buckling due to external actions (O'Rourke, EERI and So, 2000; Cozzani *et al.*, 2010). Post-earthquake damage observations show that a very common type of failure is elephant foot buckling (EFB), that is a plastic deformation at the base of the shell due to excessive concentration of meridional compressive stress. This type of damage is considered, in many studies (Salzano, Iervolino and Fabbrocino, 2003; Iervolino, Fabbrocino and Manfredi, 2004; Bakalis, Vamvatsikos and Fragiadakis, 2017), as one of the structural damage states that can cause rapid release of liquid content.

Fragility functions for atmospheric storage tanks subjected to ground shaking are widely studied in the literature and have been derived both with empirical and analytical approaches. Some of the available analytical approaches use simplified surrogate models for tank dynamic behaviour and often consider EFB as one of the principal failure criteria (Iervolino, Fabbrocino and Manfredi, 2004; Bakalis, Vamvatsikos and Fragiadakis, 2017). Empirical approaches employ records of damages to tanks from past seismic events (O'Rourke et al., 2000; Salzano et al., 2003). Specifically, in the work of Salzano and co-authors, different anchorage conditions and filling level of the tanks are taken into account, with different fragility functions provided for anchored and unanchored, half-full or almost-full tanks. (Iervolino, Fabbrocino and Manfredi, 2004) propose an analytical approach for deriving the fragility functions for unanchored atmospheric storage tanks considering as failure criterion only the EFB. For the purposes of the present study, the fragility models considered are those proposed in the latter work for anchored tanks and the various filling levels. This is mainly motivated by the fact that, in that empirical approach, the release-of-contents limit state was explicitly considered as part of the observed damage dataset. Theses fragility models are assumed to follow log-normal distributions with medians *pga* (μ) and logarithmic standard deviations (β) reported in Table 1 (note that these two parameters can be interpreted as the median and standard deviation of the logarithm of the *pga* causing failure). In order to facilitate comparison with the case of tsunami risk, in addition to these two fragility curves, it is also assumed that tanks which are very nearly empty have a negligible probability of reaching this damage state from ground shaking, due to the absence of moving liquid mass; this simplification is corroborated by historical earthquake damage data for storage tanks, showing no recorded occurrence of catastrophic failure under a degree of filling level less than of 50%. The filling level (ψ) of the tank is defined as the ratio between the level of the internal liquid (h_f) and the maximum safe filling level $H_{f,max} < H$ determined by the floating roof's end-of-course stop provided by the top stiffening ring.

Table 1. Parameters of log-normal distribution of seismic fragilities (Salzano, Iervolino and Fabbrocino, 2003).

Filling condition	$\boldsymbol{\mu}$ **[g]**	$\boldsymbol{\beta}$
Half full	3.72	0.80
Near full	1.25	0.65

On the other hand, this case-study uses fragility functions for the same type of tanks subjected to tsunami that were previously developed by the same authors (Vitale, 2024), using non-linear numerical structural models and a simplified quasi-static representation of the tsunami-induced pressures acting on the vessels (ASCE7, 2017). These analytical fragilities considered three failure mechanisms that could lead to content release: (i) buckling of the cylindrical shell wall due to compressive circumferential stresses, induced by the pressure difference between the tsunami external pressure and the internal hydrostatic pressure of the vessel's contents, (ii) lateral displacements due to lateral hydrodynamic forces exerted by the tsunami overcoming the shear resistance of the anchors and also friction, and (iii) excessive displacements due to axial tension failure of the anchors due to buoyant forces. These three mechanisms are schematically illustrated in Fig.2. It is assumed that activation of at least one of these failure mechanisms will likely cause leakage due to rupture of connections with piping systems. The uncertainties in structural properties considered in the fragility derivation include the axial and shear resistance of the anchors, and the level of geometric fabrication imperfections of the tank shell that drives stability. The fragility model was derived based on numerical results from finite element models of archetype tanks for the elastic stability of the cylindrical shell and Monte-Carlo simulation of progressive collapse for the anchorage-related failure models. A series of parametric models were then fitted to the calculated failure probabilities, given below. The interested reader can find more details in available documentation (Vitale, 2024).

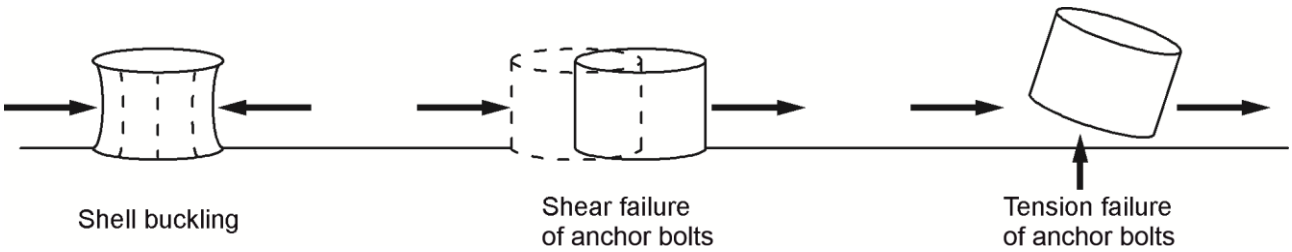

Fig.2. Schematic representation of structural failure modes considered.

According to this fragility model, the probability of failure given tsunami height and filling level, $P[F|\phi,\psi]$, is given by Equation (1):

$$\begin{cases} P[F|\phi,\psi] = 1 - \prod_{i=1}^{3}(1 - P_i[F|\phi,\psi]) \\ P_i[F|\phi,\psi] = 1 - e^{-\left(\frac{\phi}{a_i(\psi)}\right)^{b_i(\psi)}} \end{cases}, \quad (1)$$

where $\phi = h_w/H_{f,max}$ is the normalized tsunami intensity and $P_i[F|\phi,\psi]$, with $i = 1,2,3$, are Weibull cumulative distribution functions corresponding to the conditional probability of activation of each of the three failure mechanisms, with $a_i(\psi)$ and $b_i(\psi)$ being their scale and shape parameters, respectively. The subscript is used with $i = 1$ corresponding to shell buckling, $i = 2$ to tensile failure of the anchors and $i = 3$ to sliding after their shear failure. Table 2 shows the dependence of the Weibull parameters on normalized filling level ψ for the three tank geometries considered.

Table 2. Parameters of the Weibull distribution for tsunami fragilities.

Tank	**Shell buckling**		**Tensile failure of anchor bolts**		**Shear failure of anchor bolts**	
Slender	a_1	$0.59 \cdot \psi + 57.25$	a_2	$0.69 \cdot \psi + 35.49$	a_3	$\begin{cases} 149.92 & \psi < 45\% \\ 0.69 \cdot \psi + 119.26 & \psi \geq 45\% \end{cases}$
	b_1	$2.65 \cdot 10^{-5} \cdot \psi^3 + -2.09 \cdot 10^{-3} \cdot \psi^2 + +0.12 \cdot \psi + 5.47$	b_2	$-2.30 \cdot 10^{-3} \cdot \psi^2 + +0.33 \cdot \psi + 16.88$	b_3	$\begin{cases} 3.20 & \psi < 39\% \\ 5.70 \cdot 10^{-3} \cdot \psi + 2.98 & \psi \geq 39\% \end{cases}$
Intermediate	a_1	$067 \cdot \psi + 23.69$	a_2	$0.67 \cdot \psi + 19.90$	a_3	$\begin{cases} 139.92 & \psi < 43\% \\ 0.65 \cdot \psi + 112.23 & \psi \geq 43\% \end{cases}$
	b_1	$0.19 \cdot \psi + 6.48$	b_2	$-6.60 \cdot 10^{-3} \cdot \psi^2 + +1.45 \cdot \psi + 25.65$	b_3	$\begin{cases} 3.40 & \psi < 41\% \\ 0.01 \cdot \psi + 2.99 & \psi \geq 41\% \end{cases}$
Squat	a_1	$0.66 \cdot \psi + 10.15$	a_2	$0.67 \cdot \psi + 11.82$	a_3	$\begin{cases} 145.74 & \psi < 45\% \\ 0.76 \cdot \psi + 111.38 & \psi \geq 45\% \end{cases}$

b_1	$0.42 \cdot \psi + 9.00$	b_2	$-0.01 \cdot \psi^2 + 4.44 \cdot \psi + 35.31$	b_3	$\begin{cases} 3.69 & \psi < 44\% \\ 0.01 \cdot \psi + 3.01 & \psi \geq 44\% \end{cases}$

Fig.3 shows the fragility curves of the three archetypal tanks for 10% filling level in the upper row and 90% in the second row. In the figure, the three $P_i[F|\phi,\psi]$ curves for each case are shown in dashed lines, providing some insight into the contribution of the contemplated mechanisms to overall failure probability. In near-empty conditions, failure is governed by tension of the anchor bolts for slender tanks, while for squat tanks it is governed by shell buckling. Furthermore, shear rupture of the anchorage system only comes into play when tanks are nearly full, especially for the cases of slender and intermediate tanks. On the contrary, squat tank failure probabilities appear to be less by considerations of shear, due to the larger contact area per unit mass, leaving shell buckling as the dominant failure mode.

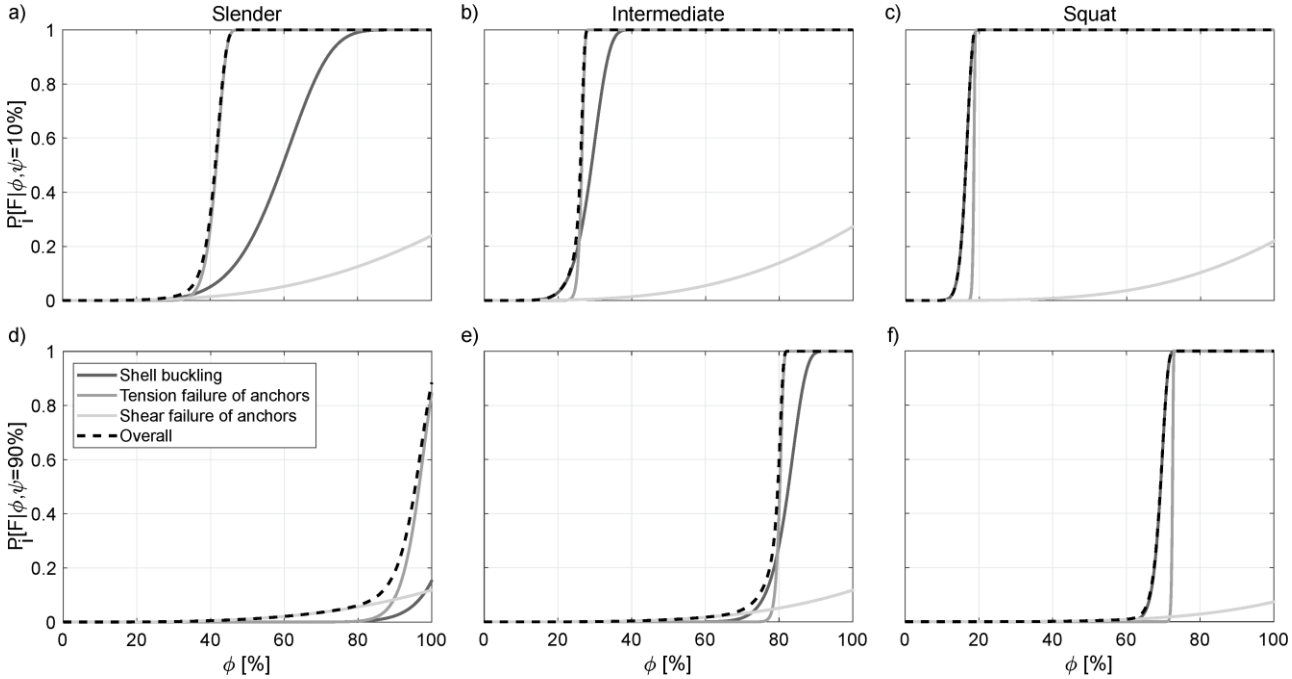

Fig.3. Tsunami fragility curves for two filling levels distinguishing the contribution of failure modes. From a) to c) fragilities for filling level of 10% for slender, intermediate and squat tanks; from d) to f) fragilities for filling level of 90% for slender, intermediate and squat tank.

While both seismic and tsunami fragilities depend on the filling level, that condition is generally uncertain during the occurrence of a natural hazard event affecting the site. Therefore, it may be useful to treat the degree of filling as a random variable and calculate the probability of failure according to Equation (2):

$$P[F|im] = \int_{\psi_{min}}^{\psi_{max}} P[F|im,\psi] \cdot f_\Psi(\psi) \cdot d\psi \qquad (2)$$

where $f_\Psi(\psi)$ is the probability density function of the filling level, in this case assumed to correspond to that of a uniform distribution (UD). The results of this operation are shown in Fig.4 for both the seismic and tsunami fragility case. From the figure emerges that, for a given level of intensity, failure probability against tsunami increases the emptier that tank, while in the seismic case, the opposite is opposite is true, which is to be expected.

3 Multi-hazard risk results

The risk is evaluated in terms of structural failure rate λ_f that represents the mean annual number of events causing structural damage followed by contents release. For either type of natural hazard considered, λ_f can be calculated by integrating the product between the fragility curve and the absolute value of the derivative of the hazard curve, $|d\lambda_{im}|$, over all levels intensity, as per Equation (3):

$$\lambda_f = \int_0^{+\infty} P[F|im] \cdot |d\lambda_{im}| \quad (3)$$

which implies that either a specific filling level ψ has been assumed, or a probability distribution thereof, according to Equation (2). The results of this operation for the case-study site and atmospheric tank geometric configurations are shown in Table 3 for the seismic case and in Table 4 for the tsunami case.

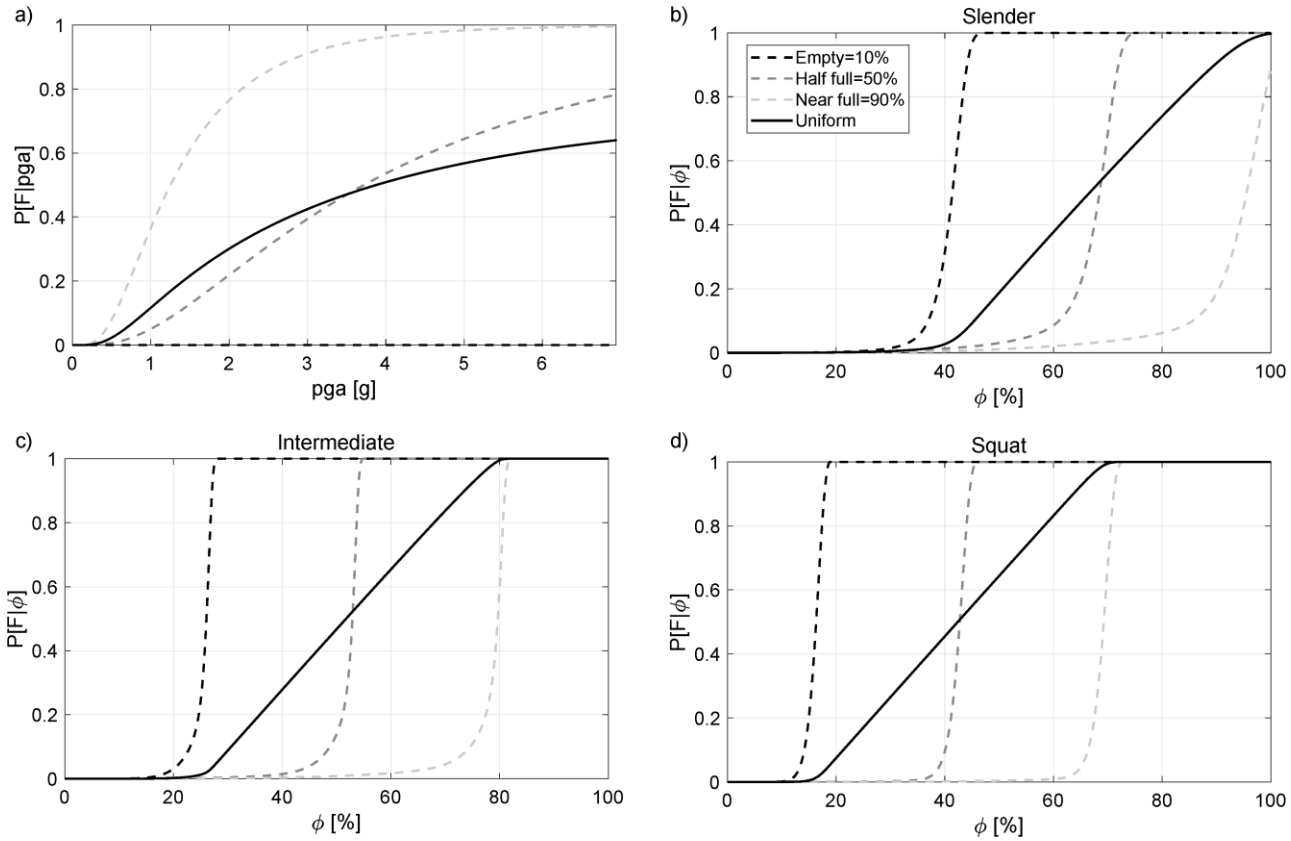

Fig.4. Fragility curves for three filling levels and for uniform distribution of the filling levels. a) Seismic fragility curves; from b) to d) tsunami fragility curves, respectively for slender, intermediate, and squat tanks.

Table 3. Structural failure rates for seismic ground-shaking event.

Earthquake	
Filling level	λ_f
10%	0 (assumed)
50%	6.82E-05
90%	5.45E-04
UD	1.70E-04

Table 4. Structural failure rates for tsunami event.

Tsunami	λ_f		
Filling level	**Slender**	**Intermediate**	**Squat**
10%	5.40E-07	1.20E-06	2.83E-06
30%	1.13E-07	1.15E-07	1.55E-07
40%	6.79E-08	2.70E-08	1.08E-08
50%	5.13E-08	1.54E-08	3.26E-09
90%	1.85E-08	3.58E-09	3.94E-10
UD	1.02E-07	1.33E-07	2.48E-07

As anticipated from the discussion on the fragility functions, the influence of filling level on risk of anchored tanks, for the two types of events, moves in opposite directions: the failure rate increases with increasing filling level, in the case of earthquakes and vice versa, for tsunami. This trend could be peculiar to code-conforming seismically designed anchored tanks, where the anchorage system possesses adequate strength against shearing and buoyant forces. This because, when the tanks are near-empty, the governing failure mode against tsunami actions, appears to be elastic buckling due to compressive radial stresses that are unlikely to have been contemplated during the steel shells' design. As the tanks get progressively fuller, the internal pressure countermands the external imposed by the tsunami, but the fragility against major lateral or upwards displacement is less than against the unforeseen external pressure, due to the code-conforming anchorage system, ostensibly designed to carry seismic base shear. However, still for the case of tsunami loading, the failure rate is also influenced by tank slenderness. The results indicate that for filling levels up to 30%, the failure rate increases from slender to squat, while for filling levels greater than 40% slender tanks appear more vulnerable. On the other hand, a full tank under seismic ground motion will experience higher meridional compressive stresses near the base due to larger overturning moments from the inertial effects of the moving liquid, thus favouring EFB type of failure.

In addition to failure rates for specific filling levels, the table also provides the failure rates associated to a uniform distribution of Ψ. In this example, choosing as the minimum and maximum filling level $\psi_{min} = 0.10$ and $\psi_{max} = 0.90$, respectively, with the mean being $\bar{\psi} = 0.50$. The results show that the failure rates obtained from marginalizing the distribution with respect to Ψ are up to one order of magnitude larger than the λ_f associated to that mean, for both the seismic and tsunami case. This shows the importance of obtaining the fragility models with filling level as a parameter, since a first order approximation may not be adequate.

Finally, it can be observed that, for this specific site, seismic failure rates largely overshadow those from tsunami, with the former being of the order of magnitude of 10^{-5} or 10^{-4}, while the latter between 10^{-10} and 10^{-6}. However, it should be noted that this difference depends on the two site-specific hazards at the site for the two types of natural event, so the predominance of one over the other is not a result that can be generalized.

4 Conclusions

This paper preliminarily presents a series of case-study risk calculations for anchored atmospheric storage tanks exposed to both earthquake-induced ground shaking and potential tsunami. The risk is assessed, in a NaTech context, as structural failure rate, that is the mean annual number of events causing structural damage that can lead to the release of hazardous substances of these industrial units. To carry out such a risk analysis, which can be part of a broader multi-hazard QRA, one needs at least the hazard at the site of interest from PSHA and PTHA, and fragility models of the structures examined, against both natural hazards, with the latter often posing more of a challenge than the former. An application of this type of risk assessment is performed for a case study of a hypothetical waterfront refinery in Southern Italy, considering a variety of tank geometries. For this site, some of the required models are taken directly from existing literature, that is the tsunami hazard and seismic fragility, while the seismic hazard and tsunami fragility were previously developed by the same authors (Vitale, 2024) and were briefly presented here.

The results highlight that the selected risk metric depends on the filling level that the tanks are found in, as well as on the aspect ratio of the tanks, with different tsunami-induced failure mechanisms becoming prevalent for different tank geometries. More specifically, failure rates due to ground shaking tend to increase as the tanks are considered progressively fuller, while the opposite trend was observed for the case of tsunami-induced failure. The results show that, when filling level is treated as a random variable and all levels are considered equally likely, a first order approximation for risk obtained by using only the expected value of the liquid content level, results in lower risk estimates than the more accurate calculation, by almost an order of magnitude, for both seismic and tsunami cases. The results also show that, in the case of tsunami events, the effects of tank slenderness and filling grade on their vulnerability are intertwined, with squat tanks being more vulnerable than slender or intermediate ones for filling levels up to 30%, after which the trend is reversed. This series of case studies offers some insights that can be useful in the context of a multi-hazard NaTech quantitative risk assessment for industrial plants.

5 Acknowledgements

The study presented in this article was developed within the RETURN “Multi-risk science for resilient communities under a changing climate” (PIANO NAZIONALE DI RIPRESA E RESILIENZA (PNRR), Mission 4, Component 2, Investment 1.3 – D.D. n.341 15/3/2022, PE0000005); and PRIN 2017 *Assessment of Cascading Events triggered by the Interaction of Natural Hazards and Technological Scenarios involving the release of Hazardous Substances* funded by the Italian Ministry of Universities and Research.

6 References

API 650 (2018) *American Petroleum Institue, Welded Tanks for Oil Storage*.

ASCE7 (2017) *Minimum design loads and associated criteria for buildings and other structures*, *Minimum Design Loads and Associated Criteria for Buildings and Other Structures*. American Society of Civil Engineers (ASCE). Available at: https://doi.org/10.1061/9780784414248.

Bakalis, K., Vamvatsikos, D. and Fragiadakis, M. (2017) ‘Seismic risk assessment of liquid storage tanks via a nonlinear surrogate model’, *Earthquake Engineering & Structural Dynamics*, 46. Available at: https://doi.org/10.1002/eqe.2939.

Basco, A. and Salzano, E. (2016) ‘The vulnerability of industrial equipment to tsunami’, *Journal of Loss Prevention in the Process Industries*, 50. Available at: https://doi.org/10.1016/j.jlp.2016.11.009.

Center for Chemical Process Safety (CCPS) (2010) ‘Chemical Process Quantitative Risk Analysis’, in *Guidelines for Chemical Process Quantitative Risk Analysis*, pp. 1–55. Available at: https://doi.org/https://doi.org/10.1002/9780470935422.ch1.

Cornell, C.A. (1968) ‘Engineering Seismic Risk Analysis.’, *Bulletin of the Seismological Society of America*, 58, pp. 1583–1606.

Cozzani, V. *et al.* (2010) ‘Industrial accidents triggered by flood events: Analysis of past accidents’, *Journal of Hazardous Materials*, 175(1), pp. 501–509. Available at: https://doi.org/https://doi.org/10.1016/j.jhazmat.2009.10.033.

Iervolino, I., Fabbrocino, G. and Manfredi, G. (2004) *Fragility of standard industrial structures by a response surface based method*, *Journal of Earthquake Engineering*.

Lees, F. and Lees, F.P. (2005) *Lees’ Loss Prevention in the Process Industries : Hazard Identification, Assessment and Control*. Burlington, UNITED STATES: Elsevier Science & Technology. Available at: http://ebookcentral.proquest.com/lib/unina-ebooks/detail.action?docID=294229.

O’Rourke, M., EERI, M. and So, P. (2000) ‘Seismic Fragility Curves for On-Grade Steel Tanks’, *Earthquake Spectra - EARTHQ SPECTRA*, 16(4), pp. 801–815. Available at: https://doi.org/10.1193/1.1586140.

Salzano, E., Iervolino, I. and Fabbrocino, G. (2003) ‘Seismic risk of atmospheric storage tanks in the framework of quantitative risk analysis’, *Journal of Loss Prevention in the Process Industries*, 16(5), pp. 403–409. Available at: https://doi.org/https://doi.org/10.1016/S0950-4230(03)00052-4.

UNI EN 1993-1-8 (2005) ‘Eurocode 3 - Design of steel structures - Part 1-8: Design of joints’. Available at: https://store.uni.com/en/uni-en-1993-1-8-2005 (Accessed: 12 November 2022).

UNI EN 1993-4-2 (2017) ‘Eurocode 3, Design of steel structures - Parte 4-2: Tanks, UNI EN 1993-4-2:2017’. Available at: https://store.uni.com/uni-en-1993-4-2-2017 (Accessed: 8 September 2022).

UNI EN 1998-4 (2006) ‘Eurocode 8 - Design of structures for earthquake resistance - Part 4: silos, tanks and pipelines’. Available at: https://store.uni.com/en/uni-en-1998-4-2006.

Vitale, A. (2024) *Earthquake and Tsunami multi-hazard risk analysis of a petrochemical plant*. PhD Thesis in Ingegneria Strutturale Geotecnica e Rischio Sismico. Tutors: Iunio Iervolino, Georgios Baltzopoulos, Pasquale Cito. Università degli Studi di Napoli Federico II.

Volpe, M. *et al.* (2019) 'From regional to local SPTHA: Efficient computation of probabilistic tsunami inundation maps addressing near-field sources', *Natural Hazards and Earth System Sciences*, 19(3), pp. 455–469. Available at: https://doi.org/10.5194/nhess-19-455-2019.